

# Synthesis and characterization of electrodeposited hierarchical nanodendritic NiCoFe alloy powders

L. D. Rafailović<sup>1,2</sup>, C. Gammer<sup>2</sup>, C. Kleber<sup>1</sup>, C. Rentenberger<sup>2</sup>, P. Angerer<sup>1,3</sup>, H. P. Karnthaler<sup>2</sup>

<sup>1</sup> *CEST, Center of Electrochemical Surface Technology, Viktor-Kaplan- Strasse 2,*

*2700 Wr. Neustadt, Austria*

<sup>2</sup> *University of Vienna, Physics of Nanostructured Materials, Boltzmannngasse 5,*

*1090 Vienna, Austria*

<sup>3</sup> *present address: Materials Center Leoben, Roseggerstrasse 12, 8700 Leoben, Austria*

**Please cite as:** Journal of Alloys and Compounds 543 (2012) 167

<http://dx.doi.org/10.1016/j.jallcom.2012.07.081>

## Abstract

Ternary Ni<sub>50</sub>Co<sub>30</sub>Fe<sub>20</sub> powders with an open dendritic structure were made by electrodeposition. The diffusion controlled deposition allows fabrication of alloy powders with a composition corresponding to that of the electrolyte. Their morphology was studied by electron microscopy methods revealing that the particles have a highly branched dendritic structure extending from the micrometer scale to the nanoscale containing a high density of defects as grain boundaries and twin boundaries. We propose that this structure forms by massive repeated nucleation far off thermodynamical equilibrium at a high current density under strong hydrogen bubble evolution. The nanodendritic structure could be of interest for practical applications due to their high density of active sites and high surface area. The powders are envisioned for electrochemical applications.

**Keywords:** nanostructured materials, crystal growth, grain boundaries, transmission electron microscopy, TEM

## 1. Introduction

Considerable work has been done in the field of iron group thin films and compact deposits [1], but systematic studies on electrodeposition of open, dendritic structures and alloy powders are still lacking despite the wide range of potential applications. High surface area materials [2] and their significantly increased electrocatalytic [3,4] have drawn attention of researchers in the field of electrochemical energy devices [5]. The recent electrochemical approach where the hydrogen bubble evolution promotes electrodeposition of size dependent nickel nanoparticles [6] is an interesting addition to the currently used production techniques for powders like mechanical processing, chemical reactions or liquid metal atomization. Of particular interest is the study of nanostructured materials due to their unique physical properties originating from the high density of grain boundaries [7-9]. Recently, significant attention has

---

<sup>1</sup> Corresponding author, Tel.:+43 2622 222 66-26; fax:+43 2622 222 66-50  
E-mail address: [lidija.rafailovic@univie.ac.at](mailto:lidija.rafailovic@univie.ac.at) (L.D.Rafailovic)

been devoted to the investigation of open nanostructures [10,11] obtained within a specific electrochemistry regime (i.e. high overpotential or current density) and using hydrogen bubbles as a dynamic template for production of foams [12]. In an overview of the different surface morphologies that can be achieved by electrodeposition it is stated that formation of dendritic structures selectively occurs at structural defects as growth sites [13]. It was recently shown that open, porous foams exhibit significantly enhanced reaction rates [12]. Promising applications of these materials in the field of energy storage with increased reaction rates can originate from their unique microstructure. The aim of the present paper is the synthesis of NiCoFe alloy powder made by electrodeposition and their detailed microstructural characterization. Therefore, composition, phase, nanostructure, size and morphology of the electrochemically obtained particles are studied using a combination of experimental methods: scanning electron microscopy (SEM), transmission electron microscopy (TEM), X-ray diffraction analysis (XRD) and photogravimetric sedimentation to characterize the structure of the achieved nanodendritic NiCoFe alloy powders.

## 2. Experimental procedures

The NiCoFe alloy powder was electrodeposited on polycrystalline Ti cathodes with constant current. The powders were obtained galvanostatically at high current density of  $1 \text{ A cm}^{-2}$  at room temperature without stirring in an open glass electrochemical cell with a volume of  $1.0 \text{ dm}^3$  with a Ti sheet ( $1 \text{ cm}^2$ ) placed in the center of the cell and used as the working electrode. Flat electrolytic Ni electrodes with  $10 \text{ cm}^2$  surface area, placed at a distance of 2 cm were used as anodes. The electrolyte solutions were made from analytical grade chemicals and high purity water. The ternary NiCoFe powders were electrodeposited from solutions containing  $0.09\text{M NiSO}_4 + 0.03\text{M FeSO}_4 + 0.053\text{M CoSO}_4 + 0.4\text{M H}_3\text{BO}_3 + 0.28\text{M NH}_4\text{Cl}$ , at  $\text{pH}=2$  adjusted with HCl [14]. The powder was removed using a brush after 180 and 1800 s, respectively. The solution was discarded and replaced with fresh electrolyte after 2 h of electrolysis to prevent significant change in composition. All samples were carefully treated to prevent oxidation due to the high surface area exposed to oxygen and moisture in the air [15]. It should be noted that oxidation of the deposit is most likely to occur during washing and drying steps, not during electrodeposition in acidic electrolytes [16]. However, acids can promote oxidation during drying. Therefore, initial washing consisted of repeated rinsing with high purity water. In addition, stabilization was attempted with a colloidal substance (0.1 % benzoic acid solution), followed by washing and finally drying in a tube furnace under vacuum at  $100 \text{ }^\circ\text{C}$  for 1 hour.

The determination of the phase content and that of the crystallite size was conducted by X-ray diffraction in Bragg-Brentano geometry. Evaluations of the phase and crystallite size were done by Rietveld refinement [17] using the TOPAS software [18]. The particle size distribution of the NiCoFe alloy powder was determined by a method which combines photometric gravitation and centrifugal sedimentation based on Stokes law. The change in concentration of the suspension was detected by optical means at a fixed distance from the uppermost surface and the time measured from the commencement of the sedimentation. The measurements of powder

particle size were done using the particle size analyzer, in a glycerin based solution. The morphology was analyzed with a SEM. For the TEM study the powder was transferred on a carbon grid. TEM bright field and dark field images were taken together with electron diffraction images allowing a detailed analysis of the structure. From the evaluation of selected area electron diffraction (SAD) images by using the method of profile analysis (PASAD), data on the crystallite size can be gained [19,20]. By an analysis with the Williamson-Hall plot additional data of the defect structure can be gained that reflect information of localized areas. The data from the electron diffraction images refer to regions selected in TEM images but the results are still statistical, a fact that in the case of TEM pictures can only be achieved by evaluating a large number of them.

### 3. Results and discussions

Electrosynthesized metal powders with a high surface area can spontaneously fall off or be removed from the electrode [13]. It has been reported that depending on the composition and current density applied, it is possible to achieve CoNi alloys with different compositions and morphologies [12,15,21]. Here we show that under similar experimental conditions it is possible to electrodeposit nanodendritic ternary NiCoFe alloy powders with a given composition. The composition close to  $(\text{NiCo})_3\text{Fe}$  was selected since it has a low thermal expansion coefficient that can be useful for high temperature applications.

The chemical composition of the ternary NiCoFe alloy powder obtained at a current density of  $1 \text{ A cm}^{-2}$  and removed after 180 s was determined by energy dispersive X-ray spectroscopy yielding that its composition is  $\text{Ni}_{50}\text{Co}_{30}\text{Fe}_{20}$ , corresponding to the bath composition. The XRD measurements showed also the presence of FCC phase only; no peaks were encountered related to oxides (Fig. 1). The observation of the FCC phase agrees with the phase diagram [22] of ternary NiCoFe for the present composition that is in the range of substitutional solid solutions of Ni, Co and Fe. For the determination of the lattice constant, Ge powder was added as a standard leading to the result that the FCC NiCoFe solid solution has a lattice constant of  $a = 0.3554 \pm 0.0002 \text{ nm}$  that is similar to that of Ni. To determine the crystallite size (equivalent to the coherently scattering domain size) from the X-ray data a Rietveld refinement was carried out; all peaks were included in the calculation and the instrumental broadening was taken into account. To take care of the influence of strain a double-Voigt approach was used, separating size and strain broadening [18]. The calculations yield that the NiCoFe alloy powder has an area weighted mean crystallite size of  $7 \pm 1 \text{ nm}$ . A comparison with NiCoFe alloy powders obtained at a current density of  $1 \text{ A cm}^{-2}$  and removed after 1800 s (10 times longer) showed that the composition and the crystallite size are not changed.

To determine the morphology and the particle size of the electrodeposited NiCoFe powders, two different techniques, SEM imaging and gravitation/sedimentation methods were employed. Figure 2 shows SEM images of the alloy powder particles that exhibit a highly branched three-dimensional morphology. The powder removed after 180 s contains particles in the range of  $5\text{-}30 \mu\text{m}$  (Fig. 2a). With increasing time of powder production, the particle size of

the powder increases showing particles with dimensions larger than 100  $\mu\text{m}$  after 1800 s (Fig. 2b). Increasing the deposition time leads by self assembly to large particles with more pronounced high order branches. To determine the particle size of the powder obtained after 180 s of deposition, the sedimentation method was used. Figure 3 show the result of the particle size distribution yielding a mean size of about 10  $\mu\text{m}$ . Based on the values of the particle sizes it is possible to determine the specific surface area of the NiCoFe powder sample resulting to 0.094  $\text{m}^2\text{g}^{-1}$  for the particles electrodeposited at 180 s. It should be pointed out that this value was calculated assuming dense particles, and therefore does not take into account the fine substructures of the particles. This means that in addition to the rather large specific surface area of the particles the hierarchical dendritic morphology gives rise to an additional surface that is orders of magnitude larger, making this NiCoFe powder interesting for applications.

The combined studies by SEM and TEM images lead to the result that the electrodeposited NiCoFe powders have a hierarchical nanodendritic structure. In the SEM image (Fig. 2a) particles as large as 30  $\mu\text{m}$  containing dendritic branches of about 1  $\mu\text{m}$  are visible after deposition for 180s. In addition, the TEM bright field image (Fig. 4a) shows that particles deposited under the same condition are dendritic even on the nanoscale down to <50 nm. The corresponding TEM selected area electron diffraction image taken from an area of about 1  $\mu\text{m}^2$  is shown in Figure 4b. The diffraction image reveals a FCC structure showing no texture. To investigate on a local scale the structural homogeneity of the dendritic structure, diffraction images were taken in different areas of the sample. An evaluation of these diffraction images using the PASAD software [19] leads to the result that the powder is homogenous in structure.

Figure 4c shows a TEM bright field image taken at higher magnification. The branches consist of a nanograined structure with grains about 10-30 nm in size. The grains contain twins (cf. arrows). Complex contrast features that might lead to misinterpretations are frequently observed in nanostructured materials due to moiré effects from overlapping crystal structures (indicated by M) [23]. Therefore a careful analysis of the grains was carried out using numerous TEM dark field images. The inset in Figure 4c shows a TEM dark-field image corresponding to the region of the grain encircled in the TEM bright field image, revealing the frequent occurrence of twins. The regions lighting up in TEM dark field images show the twinned structure and not that of the grains. This means the size of the twins corresponds to that of the crystallites. Therefore, TEM dark field images were used to determine the histogram of the crystallite sizes (cf. Fig. 5). More than 500 crystallites evaluated by digital imaging processing yield a volume weighted mean value of  $10\pm 1$  nm that corresponds to an area weighted mean value of  $8\pm 1$  nm. This value is in good accordance with that obtained by XRD giving an area weighted mean crystallite size of  $7\pm 1$  nm. The results suggest that the dendrites consist of nanograins (about 20-40 nm in size) that contain up to 4 twin boundaries. In order to achieve a statistical analysis of both the grain size and the twin density TEM diffraction data were used for the evaluation. The method of PASAD was applied to carry out a profile analysis of the diffraction peaks of the diffraction rings present in the selected area diffraction images. Based on the findings of the twins as deduced from the TEM images the diffraction data were evaluated with a Williamson

Hall plot taking the occurrence of the twins into account [24] (Fig. 6). This leads to the results as follows: (i) volume weighted grain size  $18\pm 4$  nm and (ii) twin density about 2%.

From TEM and SEM investigations it is concluded that the electrochemically obtained ternary NiCoFe alloy powder shows a highly hierarchical structure with a morphology reaching over three orders of magnitude from the microstructure to the nanostructure. The particles grow with increasing deposition time reaching sizes larger than  $100\ \mu\text{m}$  while the subbranches stay as small as 50 nm. The branches themselves consist of nanograins and they are highly faceted; the nanograins contain several twins and the size of the twins corresponds to that of the crystallite size ( $< 10$  nm). In contrast to the particle size, the crystallite size does not change with increasing deposition time.

The resulting structures can be characterized by the Hausdorff fractal dimension,  $D_f$ , that is determined by digitizing photographs and taking the best-fit slope of  $\ln(N)$  vs.  $\ln(r)$ , where  $N(r)$  is number of pixels contained within a radius  $r$  [25]. Therefore, a non-fractal planar boundary (e.g. circle) would have  $D_f=1$ , whereas a highly fractal boundary such as that of the Mandelbrot set has  $D_f=2$  [26]. In practice electrochemically deposited Zn dendrites were found to exhibit  $D_f$  up to 1.85 depending on the current density [27]; it should be mentioned that natural ferns have a similar value of  $D_f$  [28]. In the present case, the evaluation of TEM images (cf. Fig.4a) with fractalyse (ver. 2.4) fractal analysis software [29] leads to a fractal dimension of  $D_f \sim 1.77$  for dendritic NiCoFe powder deposited at  $1\ \text{A cm}^{-2}$ .

In the present case the dendritic structures made by electrodeposition form under conditions far off the thermodynamic equilibrium. This leads to a high nucleation rate causing a high density of defects (grain boundaries and twin boundaries). There are reports that nanotwin formation is favored by pulse plating as compared to direct current plating. This is the case for lower current densities producing compact layers [30, 31]. In contrast we show that a nanostructure (nanograins and nanotwins) is formed by direct plating with a high current density ( $1\ \text{A cm}^{-2}$ ) at room temperature. As compared to pure Cu the low stacking fault energy of the ternary NiCoFe alloy will also enhance the formation of nanotwins [8]. The increased current density during deposition leads to an increased overpotential and therefore to the formation of a large number of metal nuclei on the cathode surface. The growth of the nanocrystals is periodically interrupted by the periodic hydrogen bubble evolution and coalescence. It also favors the repeated nucleation leading to an open dendritic structure.

It is also interesting to note that many investigations of the crystallographic properties of dendrites have reported the existence of twin structures [32,33]. Also, as stated in [34,13] in the twinning process, a so-called indestructible reentrant groove is formed; repeated one-dimensional nucleation in the groove is sufficient to provide for growth extending in the direction defined by the bisector of the angle between the twin planes. The formation of a nanograined structure far off thermodynamic equilibrium (high nucleation rate at low temperature) is expected to cause a stress in the deposit that can lead by relaxation to nanotwinning in the deposit [36]. It is possible to yield massive nucleation and the formation of an open structure by choosing mass transport control with the variables of the electrodeposition

process properly (e.g.: high current density, low temperature and a bath composition with low metal salt concentration). As a consequence in the present case of NiCoFe a highly defected open nanodendritic structure of the powders has been achieved. The mass transport control allows depositing a homogeneous alloy with a composition corresponding to that of the electrolyte. This is in contrast to electrodeposited iron group thin films and compact deposits.

It is shown in the literature that nanotwinned dendrites of Pd prepared by electrodeposition exhibit an exceptionally high catalytic activity due to the presence of a high density of surface steps by providing active sites for the catalytic reaction that lead to an enhanced reaction rate [9]. Therefore, the nanotwinned hierarchical dendritic NiCoFe alloy powders resulting from this study could be used for applications in electrochemical devices such as batteries.

#### **4. Conclusions**

In summary we show: (i) Ternary Ni<sub>50</sub>Co<sub>30</sub>Fe<sub>20</sub> alloy powders with a FCC structure are obtained by galvanostatic electrodeposition at a high current density of 1 A cm<sup>-2</sup>. The composition of the powders corresponds to that of the electrolyte. (ii) The particle size of the NiCoFe alloy powders increases with increasing time of powder production whereas the crystallite size does not change. (iii) SEM and TEM methods show that the powder particles have a highly branched open dendritic structure extending from the micrometer scale down to the nanoscale with sub-branches smaller than 50 nm leading to the result that nanodendritic powders with a high surface area are achieved. (iv) In addition to the open hierarchical dendritic structure the powders contain a high density of stable defects (both grain boundaries and twin boundaries). Therefore it is proposed that the achieved NiCoFe powders are suitable for practical applications in electrochemical devices such as batteries.

#### **Acknowledgement**

This research was supported by the research project "Bulk Nanostructured Materials" within the research focus "Material Science" of the University of Vienna and by the Austrian Science Fund (FWF): [S10403, P22440]. The work at CEST was supported within the COMET program by the Austrian Research Promotion Agency (FFG) and the government of Lower Austria.

#### **References**

- [1] D. Kim, D. Park, B. Yoo, P. Sumodjo, N. Myung, *Electrochim. Acta* 48 (2003) 819-830.
- [2] J. N. Tiwari, R. N. Tiwari, K. Lin, *ACS Applied materials and Interfaces* 2 (2010) 2231-2237.
- [3] J. N. Tiwari, R. N. Tiwari, K. Lin, *Nano Res.* 4 (2011) 541-549.
- [4] J. N. Tiwari, F. M. Pan, T.M. Chen, R.N. Tiwari, K. L. Lin, *J. Power Sources*, 195 (2010) 729-735.
- [5] J. N. Tiwari, R. N. Tiwari, K. S. Kim, *Progress in Material Science* 57(2012) 724-803.
- [6] M. Zach, R. Penner, *Adv. Mater.* 12 (2000) 878-883.

- [7] O.V. Cherstiouk, A.N.Gavrilov, L.M. Plysova, I.Yu. Molina, G.A. Tsirlina, E.R. Savinova, J. Solid State Electrochem. 12 (2008) 497-509.
- [8] I. Kasatkin, P. Kurr, B. Kniep, A. Trunschke, R. Schlögl, Angewandte Chem. 119 (2007) 7465-7468.
- [9] S.Patra, B. Viswanath, K.Barai, N. Ravishankar, N. Munichandraiah, ACS Appl. Mater. Interfaces 2 (2010) 2965-2969.
- [10] H.C. Shin, J. Dong, M. Liu, Adv. Mater. 15 (2003) 1610-1614.
- [11] S. Cherevko, C.H.Chung, Electrochem. Commun. 13 (2011) 16-19.
- [12] LD. Rafailovic, C .Gammer, C . Rentenberger, C . Kleber, AH.Whitehead, B. Gollas, HP. Karnthaler. Phys. Chem. Chem. Phys. 14 (2012) 972-980.
- [13] S. Djokić (editor), Modern Aspects of Electrochemistry Volume 54 Electrochemical Production of Metal Powders, Springer, 2012.
- [14] Y. Sverdlov, Y. Rosenberg, Y. I. Rosenberg, R. Zmood, R. Erlich, S. Natan, Y. Shacham-Diamand, Microelectronic engineering 76 (2004) 258-265.
- [15] V. Jovic, B. Jovic, M. Pavlovic, Electrochim. Acta 51(2006) 5468-5477.
- [16] M. Pavlovic, L. Pavlovic, I. Doroslovaki, N. Nikolic, Hydrometallurgy 73 (2004) 155-162.
- [17] H. Rietveld, Journal of Applied Crystallography 2 (1969) 65-71.
- [18] Bruker AXS, TOPAS V3. General profile and structure analysis software for powder diffraction data, Karlsruhe, 2005.
- [19] C. Gammer, C. Mangler, C. Rentenberger, H.P. Karnthaler, Scripta Mater. 63 (2010) 312-315.
- [20] C. Gammer, C. Mangler, H.P. Karnthaler, C. Rentenberger, Microscopy and Microanalysis 17 (2011) 866-871.
- [21] L. D. Rafailovic, D. Minic, HP. Karnthaler, J.Wosik, T. Trisovic, G. Nauer, J. Electrochem. Soc. 157 (2010) 295-301.
- [22] Y. Yoo, Q. Xue, Y. Chu, S. Xu, U. Hangen, H. Lee, W. Stein, X. Xiang, Intermetallics 14 (2006) 241-247.
- [23] C. Rentenberger, T. Waitz, H.P Karnthaler, Scripta Mater. 51 (2004) 789-794.
- [24] T. Ungar, A. Revesz, A. Borbely, J. Appl. Cryst. 31 (1998) 554-558.
- [25] R. Brady and R. Ball, Nature 309(1984) 225–229.
- [26] M. Shishikura, The Annals of Mathematics, 147(1998) 225–267.
- [27] C. Chen and J. Jorné, J. Electrochem. Soc.137(1990)2047–2051.
- [28] Z. Ji, H. Li, Y. Liu and W. Hu, Nanotechnology 19(2008) 135602
- [29] Fractalyse Software: <http://www.fractalyse.org/>
- [30] L. Lu, Y. Shen, X. Chen, L. Qian, K. Lu, Science 323 (2009) 607-610.
- [31] G.T. Lui, D. Chen, J.C. Kuo, J. Phys.D: Appl. Phys. 42 (2009) 215410-215417.
- [32] Bechtoldt CJ, Ogburn F, Smith J (1968) J Electrochem Soc 115:813
- [33] Faust JW, John HF (1963) J Electrochem Soc 110:463
- [34] T. K. Sau (editor), A. L. Rogach (editor), Complex-shaped Metal Nanoparticles, Wiley, 2012.
- [35] D. Xu, W.L. Kwan, K. Chen, X. Zhang, V. Ozolins, K.N. Tu, Appl. Phys. Lett. 91 (2007) 023521-023526.

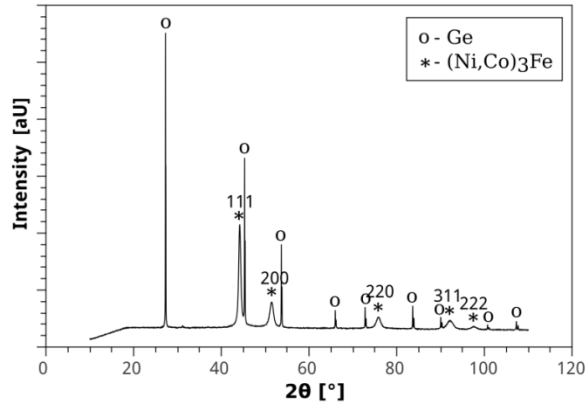


**Figure 1.** X-ray profile of the electrodeposited NiCoFe powder obtained at a current density of  $j=1 \text{ A cm}^{-2}$  and after 180s showing broad peaks. The sharp peaks correspond to the Ge standard, that was added to allow a precise determination of the lattice constant.

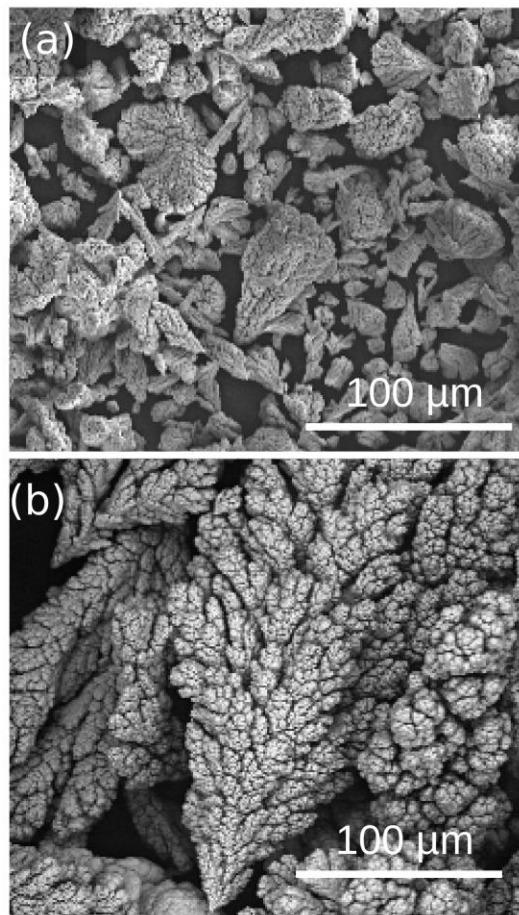


**Figure 2.** SEM images of NiCoFe powder deposited at  $j=1 \text{ A cm}^{-2}$  after (a) 180 s and (b) 1800 s deposition time. The images reveal that with increasing deposition time the particle size increases by a factor of about 10. The particles show a 3D dendritic morphology.

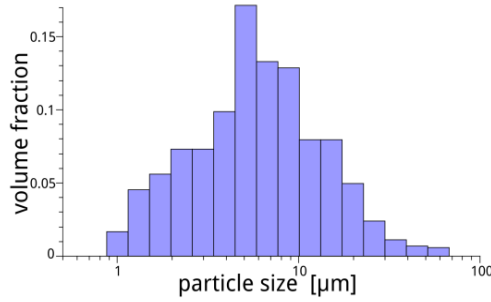


**Figure 3.** Particle size distribution of NiCoFe alloy powders ( $j=1 \text{ A cm}^{-2}$ , deposition time,  $t=180 \text{ s}$ ) measured by the sedimentation method. The distribution shows a mean of  $10 \mu\text{m}$ .

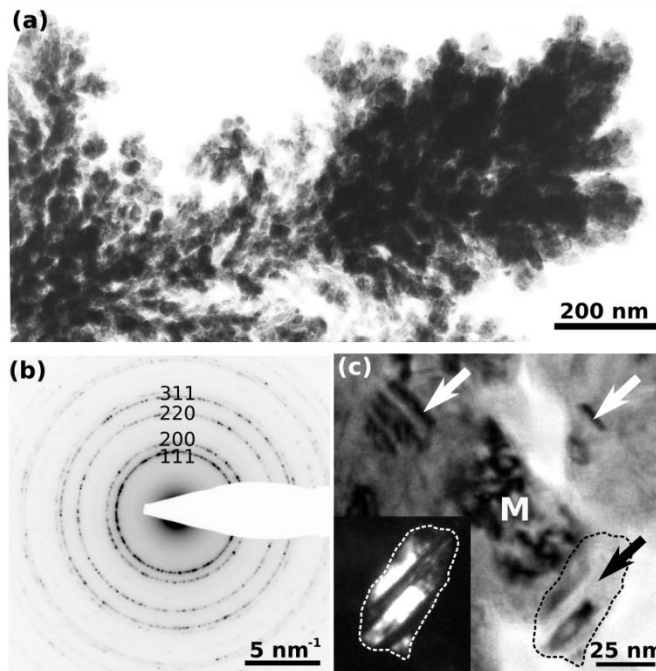


**Figure 4.** Transmission electron microscopy study of the NiCoFe powder ( $j=1 \text{ A cm}^{-2}$ , deposition time,  $t=180 \text{ s}$ ). (a) Bright-field image revealing a highly branched dendritic structure. The dendrites are very fine with branches down to less than  $50 \text{ nm}$ . (b) The corresponding electron diffraction image shows a FCC structure that is not textured. (c) Bright-field image; the branches consist of a nanograined structure with grains around  $30 \text{ nm}$  in size. The grains contain twins (indicated by arrows) as confirmed by the dark-field image showing the encircled grain (cf. inset). In the bright-field image complex contrast features caused by moiré effects from overlapping grains (M) are observed.

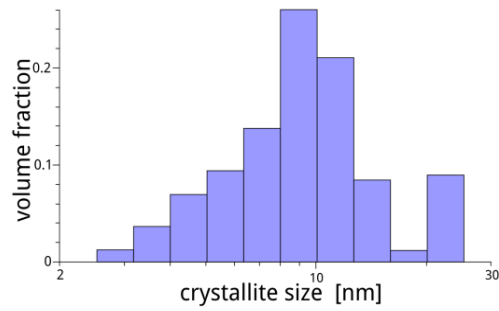


**Figure 5.** Crystallite size distribution of the NiCoFe powder ( $j=1 \text{ A cm}^{-2}$ , deposition time=180 s), determined from the contrast of the crystallites in TEM dark-field images. The distribution shows a volume weighted mean of  $10 \pm 1 \text{ nm}$ .

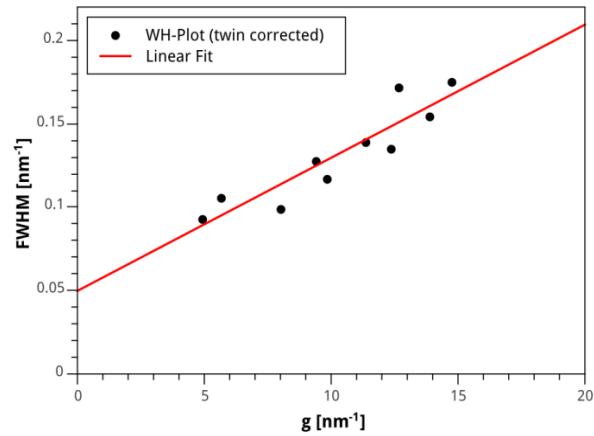


**Figure 6.** Williamson-Hall plot from the electron diffraction images of electrodeposited NiCoFe powders ( $j=1 \text{ A cm}^{-2}$ , deposition time=180 s). The full width half maximum (FWHM) values plotted as a function of the reciprocal vector  $g$  are corrected for the presence of twins according to ref [24], allowing to determine the density of the twins.